JTTEE5 12:258-264

Effect of Direct-Current Plasma Fluctuations on In-Flight Particle Parameters: Part II

J.F. Bisson and C. Moreau

(Submitted 11 December 2001; in revised form 16 April 2002)

This paper is the continuation of previous work,[1] in which plasma fluctuations were shown to produce significant time-dependent variations in the in-flight particle temperature and velocity, as well as in the number of detected particles. In this paper, the impact of the plasma fluctuations on the coating microstructure and deposition efficiency is demonstrated. Alumina coatings and deposition efficiencies, obtained with two sets of spray conditions showing similar in-flight particle conditions (velocity and temperature) with the DPV-2000 but displaying very different voltage fluctuations, are compared. The coating produced in the less stable plasma condition (C-I) is found to be more porous and contains a larger number of unmelted particles than the other coating produced in more steady plasma conditions (C-II). Moreover, condition C-I yields a significantly lower deposition efficiency. Such large discrepancies must be traced back to the physical characteristics of the particle jet. Laser illumination of the particle jet is used to probe particles too cold to be detected by pyrometric means. Cold particles are found in a much larger proportion in C-I than in C-II. They are ascribed to particles that are injected when the plasma is in a low enthalpy state. Periodic time-dependent variations in the in-flight characteristics of cold and hot particles, synchronous with the voltage fluctuations, are revealed.

Keywords alumina, control, diagnostics, microstructures, plasma fluctuations

1. Introduction

Thermal spray companies face the challenge of reducing their production cost to stay competitive and, at the same time, responding to a market pressure for increasingly demanding coating applications, to the point that some applications now require thermal spray coatings for the safe use of the coated parts. This calls for more consistency in the coating microstructure and properties. To achieve this, every aspect of thermal spray processing must be addressed, from surface preparation[2] to post-processing, through the achievement of more consistent feedstock materials,[3] the improvement of thermal spray equipment for reduced variability,[4] and the standardization of testing.[5]

Alternatives to achieving better consistency lie in the development of suitable on-line control strategies.[6] Controlling the particle jet properties using sensors is a very promising approach. Sensors[7-10] aimed at measuring the in-flight particle velocity and temperature distributions have proven especially helpful for achieving some desired coating properties[11] because they provide information on variables directly affecting the coating microstructure.[12] Maintaining these two distributions, or just their mean values, at or near a predefined set point, helps maintain coating consistency throughout the production period. But does it guarantee it?

J.F. Bisson and **C. Moreau,** National Research Council of Canada, Industrial Materials Institute, 75, De Mortagne Blvd., Boucherville, Quebec, Canada, J4B 6Y4. Contact e-mail: christian.moreau@CNRC-NRC.gc.ca.

To study that question, the following experiment was performed: two sets of spray gun parameters yielding similar in-flight particle characteristics were used to spray alumina coatings with the F4-MB gun (Sulzer-Metco, Westbury, NY). In-flight particle diagnostics were performed using the commercial in-flight diagnostics system DPV-2000 (Tecnar Automation, Ltd., St. Bruno, Canada).[13] In one condition (C-I), the current level was kept low while the secondary gas flow rate, hydrogen, was high. In the other condition (C-II), the current was raised on a high level, but the hydrogen flow rate was reduced to obtain in-flight particle values similar to the other condition. The average net power in the plasma, as obtained by subtracting the energy loss in the cooling water from the electrical power $V \cdot I$, was similar in both conditions. Moreover, temperature distributions reached by the particles in the middle of the jet were similar, and velocities were slightly different (13% difference). Details about the powder and the two sets of spray gun parameters used to produce the coating are given in Table 1. Diagnostics results are detailed in Table 2.

Hence, comparable deposition efficiencies (DE) and coating structures should be expected. However, C-I yielded a significantly lower DE (46%) than C-II (73%). Moreover, examination of a polished cross-section of each coating using conventional optical microscopy revealed very different coating microstructures. Photographs of the coatings are shown in Fig. 1(a) and (b). Lighter and round particles on the photographs were ascribed to unmelted or partially melted particles. The coating produced under condition C-I clearly has a larger number of unmelted particles trapped in the coating and also a higher porosity than the coating produced with conditions C-II. The relative number of unmelted particles in each condition was assessed by counting their numbers on each photograph. The apparent difference in porosity was confirmed by quantitative measurements on a 0.55×0.40 mm^2 coating cross-section using image analysis with Visilog software (NorPix, Inc., Montreal, Canada) using

Table 1 Equipment, Material, Spray Gun Parameters, DE, and Indications on the Microstructure for the Two Conditions Used to Produce Alumina Coatings

Condition	Value	
Gun	F4-MB	
Injection	Radial external from top	
Stand-off distance, mm	100	
Powder	Alumina (fused and crushed) PT-105C-99	
Grain size distribution, μm	−35, +15 (Microtrac) (Weight 10–90 percentile)	
Powder morphology	Fused and crushed	
Condition	C-I	C-II
Current, A	300	700
Primary gas flow rate (argon), l/min	35	35
Secondary gas flow rate (hydrogen), l/min	10	3
Carrier gas flow rate (argon), l/min	6	6
Average voltage, V	66.4	44.0
RMS voltage, V	16.4	2.7
Average brute power, kW	20	31
Average net power, kW	10	11
Deposition efficiency, %	48	73
Porosity, %	7.0	4.5
Number of unmelted particles per mm^2	450	85

Microtrac Inc., Montgomeryville, PA

standard procedure (correction for nonuniformities of lighting, thresholding, binarization, etc.).[14] The coating produced in condition C-I has a significantly higher porosity level (p = 7%) than the one produced in condition C-II (p = 4.7%). DE, porosity measurements, and an estimation of the number of unmelted particles per square millimeter for each coating are provided at the bottom of Table 1. Note that the lower velocity obtained in condition C-I (13% slower) might have contributed to some of the observed difference in the porosity and DE. Indeed, a slower particle jet usually produces a more porous coating, which is consistent with the observed differences. However, there is no such general rule regarding the relationship between in-flight particle velocity and DE.

The objective of this work is to understand why these two sets of spray gun parameters lead to different coating microstructures and DE despite having apparently comparable in-flight particle velocities and temperatures. In section two, we show that cold particle sensing using laser illumination is needed to differentiate the two in-flight particle conditions. In section three, the physical mechanism that causes one condition to display a larger number of cold particles is shown to be the plasma fluctuations. Time-resolved in-flight particle diagnostics, performed on both hot and cold particles, makes it possible to compare in-flight conditions of particles that are injected in the plasma plume at different moments corresponding to different states (i.e., temperature, velocity) of the plasma.

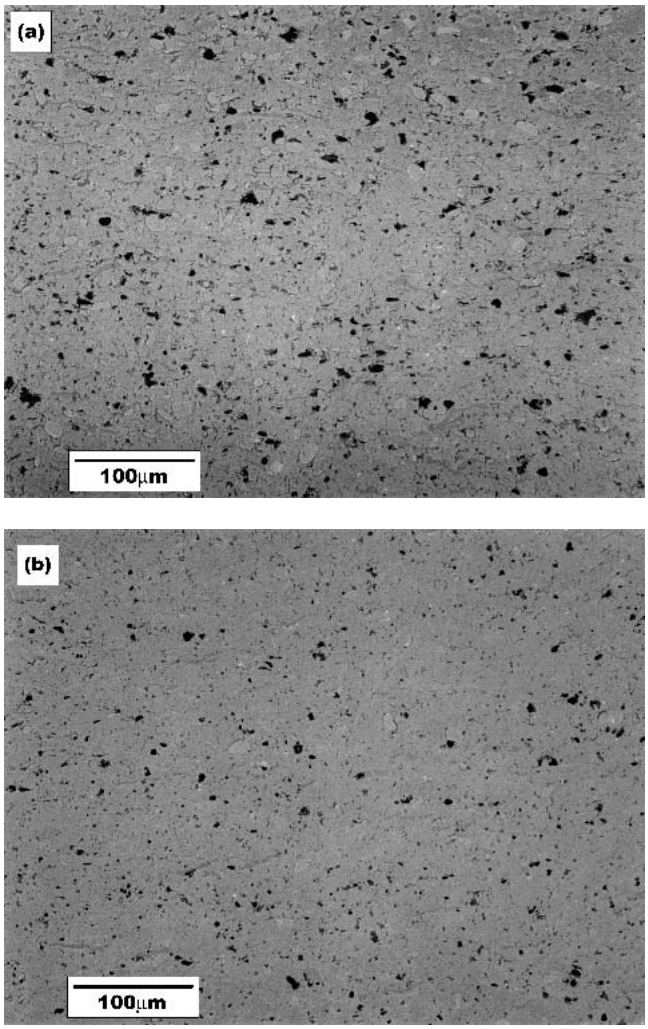

Fig. 1 Image of the coatings cross section produced in conditions **(a)** C-I and **(b)** C-II. These images were obtained using optical microscopy. A larger number of unmelted particles and a higher porosity are clearly visible in the coating C-I compared with the coating C-II.

Table 2 In-Flight Particle Diagnostics of Spraying Conditions C-I and C-II Recorded With the DPV-2000

Condition	I	II
Temperature, °C	2851	2846
σ-Temperature, °C	174	198
Velocity, m/s	274	316
σ-velocity, m/s	43	44

The diagnostics were performed at 40 mm stand-off distance.

2. Cold Particle Diagnostics

2.1 Experimental Procedure

The lower DE and larger number of unmelted particles found in coating C-I suggest that a larger number of cold particles are present in C-I than in C-II. These particles might not emit enough thermal radiation to exceed the background noise level of the detection system and, thus, might go undetected. For example, the detection limit of the DPV-2000 for a 25 μm diameter particle, with an emissivity ε = 0.4, is about 1600 °C, so 25 μm particles colder than 1600 °C are likely to go undetected. Consequently, laser illumination was used to track possible cold particles. To do so, a laser diode, emitting at a wavelength λ = 830 nm, was added to the DPV-2000 detection system to illuminate the sensor detection volume. The zone where illumination is quite uniform covers a diameter of a few millimeters and encompasses the sensor field of view. The collected backscattered light

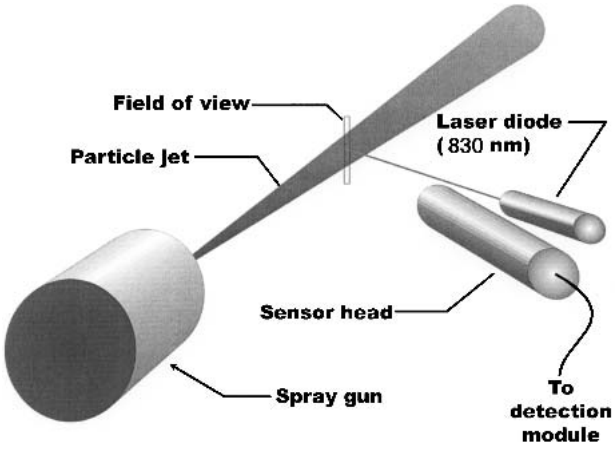

Fig. 2 Schematic view of the experimental arrangement used for cold particle sensing

from the particles is used to detect particles and measure their velocity. An illustration of the experimental set-up is shown in Fig. 2. One detector (channel A) of the sensor cabinet collects light at $\lambda = 830$ nm (mostly backscattered laser light from the particles but also some weaker radiation signal), while the other channel (B) collects only thermal radiation at $\lambda = 995$ nm. Hence two-color temperature measurements are no longer possible when laser illumination is turned on. However, "cold" and "hot" particles can be distinguished because the former generates a pulse in channel A, while no detectable thermal radiation is collected in channel B, unlike hot particles, which create a measurable radiation signal in channel B. As a second step, the laser was turned off and hot particles were characterized (temperature, velocity, and diameter) with the DPV-2000.

2.2 Results

The sensor head was scanned vertically in the particle jet and the number of "cold" and "hot" particles was measured. Comparison of Fig. 3(a) and (b) indicates that the fraction of cold particles was significant in C-I, whereas much fewer "cold" particles are present in C-II.

Examination of the temperature-diameter graph (Fig. 4) obtained in the "hot particle" mode indicates that almost all particles that are detected through their thermal emission are much more radiative than the detectivity threshold of the DPV-2000 ($T_{th} \approx 1600$ °C). Consequently, the temperature distribution of the particles sprayed in condition C-I is most likely bimodal. In effect, in view of the large number of detected cold particles, a distribution with only one peak would imply that many particles are near the detectivity limit of the DPV-2000.

These observations suggest that large time-dependent variations exist in the energy transfer between the plasma jet and the injected particles. In effect, inspection of the time-dependence of the voltage behavior substantiates this assumption. As shown in Fig. 5, condition C-I displays power fluctuations exceeding a factor of three. On the other hand, condition C-II displays much smaller fluctuations. These behaviors are in accordance with the observation from Heberlein's work,[15] which mentions that the amplitude of the arc movement increases when secondary gas flow rate is raised or when current level is reduced.

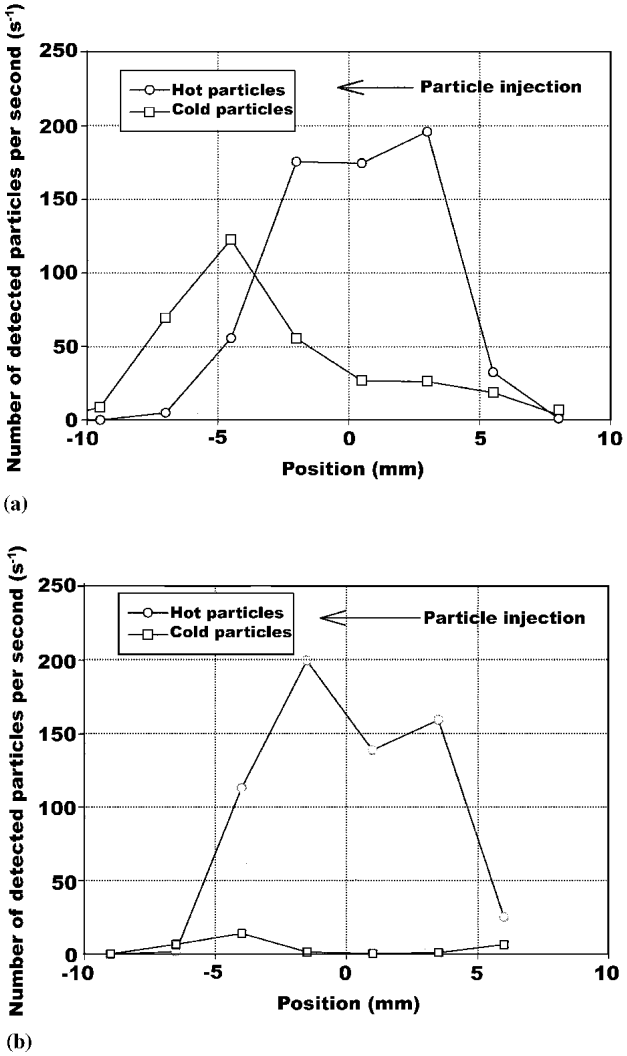

Fig. 3 Vertical scans. Comparison of the spatial distributions of cold and hot particles for conditions **(a)** C-I and **(b)** C-II

In the next section, the influence of plasma fluctuations on the in-flight particle parameters will be studied using time-resolved particle diagnostics, carried out on cold and hot particles.

3. Effect of Direct Current Plasma Fluctuations on In-Flight Particle Parameters

3.1 Experimental Procedure

In a previous paper,[1] fluctuations of the instantaneous power in the plasma plume were shown to create fluctuations of the in-flight particle parameters. A strong correlation between the instantaneous voltage and the particle velocity and temperature could be observed by using the voltage signal to trigger the acquisition of the particle radiation. The principle of operation underlying the time-resolved diagnostics is sketched in Fig. 6.

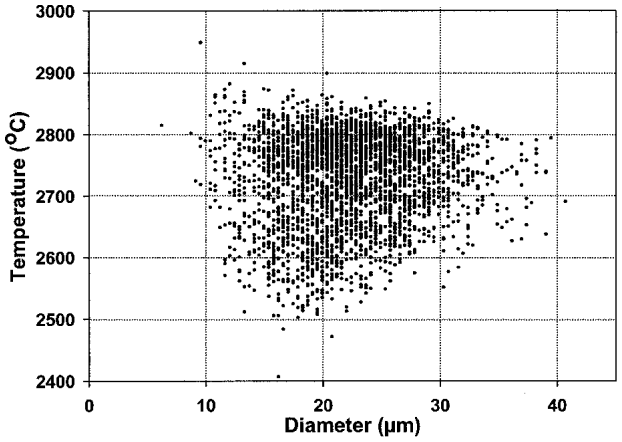

Fig. 4 Particle temperature-diameter correlation obtained in condition C-I. Almost all particles detected by thermal radiation are found significantly above the detectivity limit of the DPV-2000, which, for a 25 μm diameter particle with an emissivity, ε, of 0.4, is around 1600 °C.

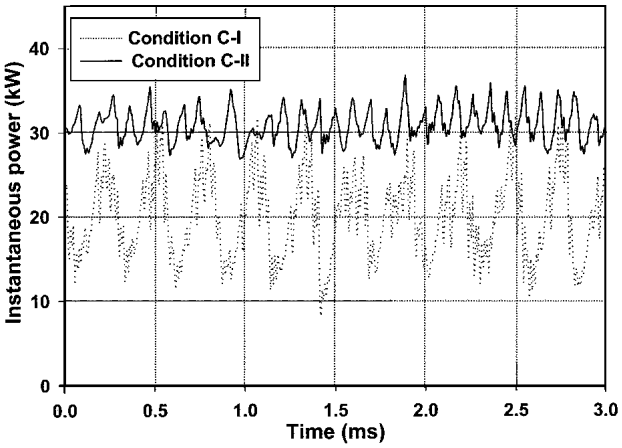

Fig. 5 Instantaneous power V · I of the two spraying conditions C-I and C-II. *V* is the voltage difference measured between the cathode and the anode and *I* is the current, controlled at a constant value.

When the torch voltage exceeds a predefined threshold, chosen close to the maximum value reached by $V(t)$, a pulse is generated by a comparator. This pulse corresponds to a moment at which the plasma reaches its highest enthalpy value. That pulse can be delayed by a predefined time delay before triggering the acquisition card of the DPV-2000. The acquisition depth was adjusted at 20 μs.[13] A particle passing in the sensor field of view during that period will eventually produce a valid particle signature enabling an evaluation of its temperature, velocity, and diameter.[16] For each time delay, the measurement is repeated until the number of analyzed particles is large enough to obtain statistically significant average values.

The fact that diagnostics is performed 40 mm away from the nozzle exit has several consequences on the interpretation of the measurements. First, particles that are detected at zero time delay after a pulse is generated from the comparator do not necessarily correspond to particles being injected when the plasma is in the highest enthalpy state, due to the time delay introduced by

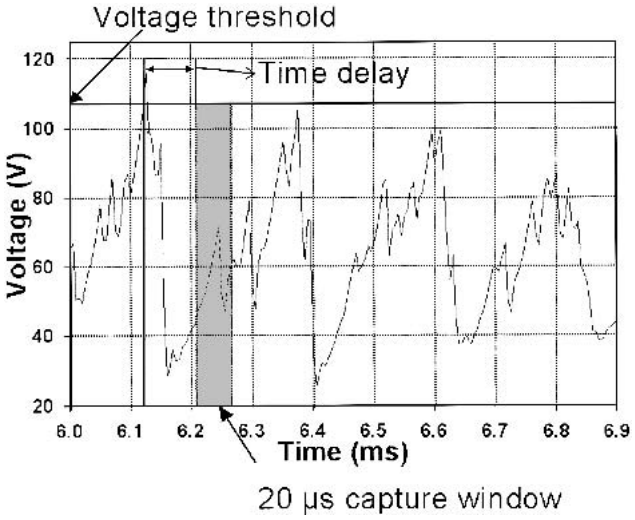

Fig. 6 Principle of operation of the synchronization of the diagnostics with the torch voltage

the time of flight of a particle from its injection point to the detection volume, 40 mm downstream. An accurate estimate of this time delay would require careful modeling of the thermal and kinetic transfers to the injected particles; it is evaluated to be on the order of 250 μs, that is, a cycle of fluctuations. Hence, the time delays in time-resolved diagnostics should be viewed in a relative sense. Moreover, for a given time delay, velocity dispersion produces time-of-flight dispersion, which in turn produces a reduction in the effective time-resolution of the diagnostics, when extrapolated at the injection point. For example, a 15 m/s standard deviation in the average velocity of 150 m/s on a 40 mm travel distance brings an uncertainty in lag time of the order of ±30 μs, which is about one tenth of a cycle. Thus, the sensor had to be placed as close to the nozzle exit as possible to reduce the impact of velocity dispersion as much as possible. Finally, it is worth noting that the applicability of this experimental procedure is largely due to the coherence of the voltage fluctuations.[1] In effect, voltage fluctuations display quasi-periodical variations (Fig. 6) that enable the reconstruction of the time-dependent average particle state on the 10^{-5} s scale, despite the fact that each particle data at some time delay arises from particles injected at different cycles of the voltage oscillations. However, the finite coherence of the voltage signal introduces some uncertainty regarding the state of the voltage extrapolated at the injection point, which in turn produces some time-resolution broadening.

3.2 Results: Hot Particle Diagnostics

Results of time-resolved diagnostics carried out for both spray conditions C-I and C-II are shown in Fig. 7(a,b), and 8. Condition C-I displays significant fluctuations in temperature and velocity during a fluctuation cycle, whereas condition C-II displays more constant values. Hotter particles detected in con-

[1]The finesse of the fundamental peak in the frequency spectrum, defined as the ratio of the frequency of the peak over its width at its half maximum value, is on the order of 5, which means that the coherence of the phase of the voltage signal is kept at least for a few cycles.

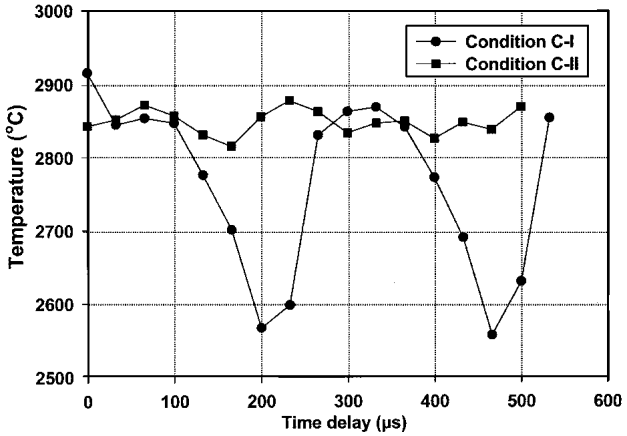

(a)

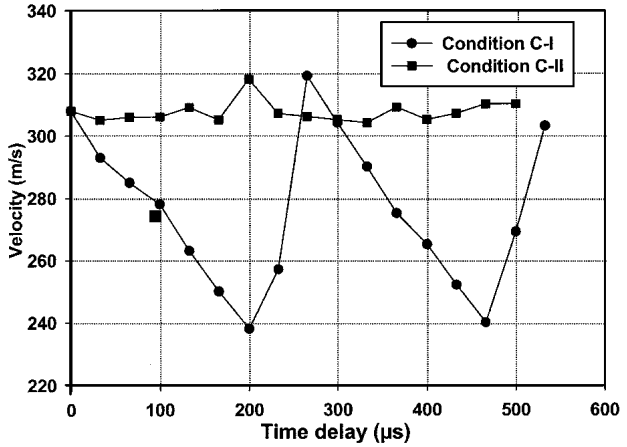

(b)

Fig. 7 Comparison of time-resolved **(a)** temperature and **(b)** velocity measurements obtained in conditions C-I and C-II. Each data point corresponds to mean values computed from samples of a few hundred of particles.

dition C-I are ascribed to particles injected when the plasma enthalpy is high, whereas colder ones are ascribed to particles injected when the plasma enthalpy is low. The observed fluctuations in the in-flight particle state suggest that each injected particle received most of its energy transfer from the plasma plume during a fraction of a fluctuation cycle. This was deliberately favored by using relatively fine and light feedstock, so that particles can be imparted high momentum.

Inspection of these graphs suggests that C-II is a hotter and faster particle condition, since values reached with C-I are almost always lower than those reached by C-II. However, inspection of Fig. 8 reveals that the number of detected colder particles, around 2600 °C, is very low. Very few particles are detected during half of a cycle. Condition C-II displays much smaller variations in the number of detected particles. This explains why the time-average temperature and velocity values, listed in Table 3, weighted by the number of detected particles, are similar in conditions C-I and C-II.

It is not clearly established yet why a quiet period arises in each cycle. One possibility is that particles do flow during that

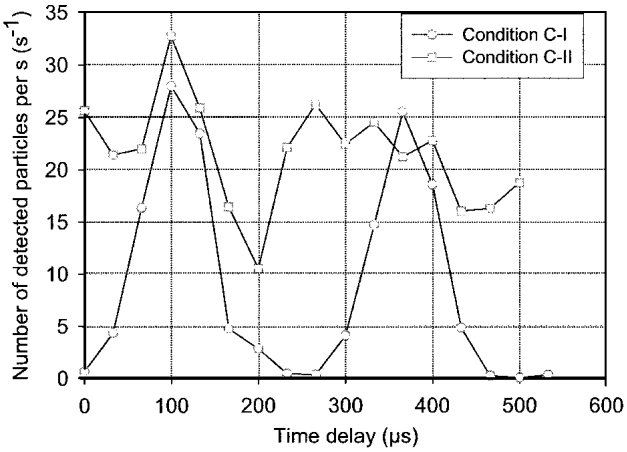

Fig. 8 Number of detected particles in conditions C-I and C-II

period but they pass undetected because they are either too cold to exceed the detection limit of the DPV-2000. Another possibility is that particles that are injected when the plasma enthalpy is low are taken up when the next hot puff of plasma comes out, giving rise to clusters or puffs of hot particles, despite the constant particle injection rate into the plasma. This seems plausible because, given their initial speed as they exit the injector (on the order of 20 m/s), the particles do not have time to bypass the nozzle exit (diameter, 5mm), during the cold part of a cycle of fluctuations, about 125 μs. A combination of the two scenarios is also possible: the proportion of cold particles (Fig. 3) seems to be inferior to what would be expected from the "duty cycle" alone (Fig. 8).

3.3 Results: Cold Particle Diagnostics

To get a more complete picture of the time-dependent particle behavior in a fluctuating plasma, time-resolved diagnostics was also performed on the cold particles using condition C-I. The diagnostics was performed using laser illumination at 40 mm from the nozzle exit and at the transverse location where the largest number of cold particles were found (Fig. 3a), that is 5 mm lower than where the maximum number of hot particles was recorded. As can be seen in Fig. 9, a cyclic time-dependent velocity is noticed, velocities ranging from 160 to 200 m/s throughout a cycle. These velocities are much lower than the 280 m/s average value measured on the hot particles. The number of cold particles detected per unit time (Fig. 10) is also modulated at the same frequency as the plasma fluctuations, but the modulation depth is much smaller than the one found for hot particles (Fig. 8). The respective phases in the evolution of the number of detected hot and cold particles cannot be directly compared (Fig. 8 and 10), since the times of flight of the hot and cold particles from the injector to the measurement volume of the DPV-2000 are different (different trajectories, different velocities). Such a comparison will need careful modeling of the energy transfer from the plasma to the particles.

4. Conclusions

Two spray gun conditions, C-I and C-II, yielding similar in-flight particle temperature and plasma enthalpy were used to

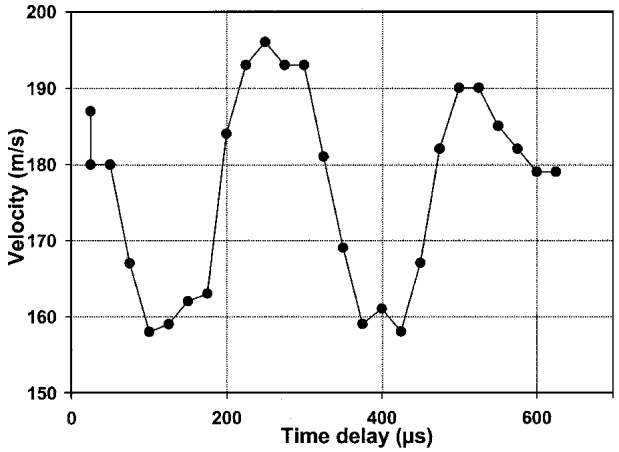

Fig. 9 Time resolved velocity of cold particles obtained in condition C-I. The velocity of the cold particles is, in average, almost half that of hot particles (cf. Fig. 7b).

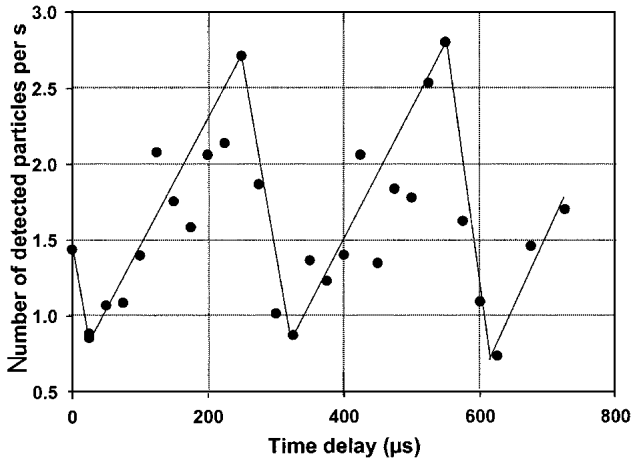

Fig. 10 Number of detected cold particles per unit time in condition C-I

produce alumina coatings. Two very different microstructures and deposition efficiencies were achieved: coating C-I displayed a lower DE, a larger number of unmelted or partially melted particles in the coating and a higher porosity. The DPV-2000 was coupled with a laser diode to see cold particles. A large number of cold particles were found in condition C-I, whereas only a few cold particles were detected in Condition C-II. The observation of voltage fluctuations in both spraying conditions revealed large cyclic voltage fluctuations for condition C-I, whereas condition C-II exhibited a more steady voltage. The combination of a large power fluctuation with low particle residence time in the plasma, due to the high particle velocity, contributed to generate a significant number of cold and slow particles in condition C-I.

Time-resolved in-flight particle diagnostics, using pyrometric detection, made it possible to see large time-dependent variations in the in-flight temperature and velocity in condition C-I, synchronous with the voltage fluctuations. Moreover, the particle detection rate was found to almost vanish for a significant portion of each cycle. The existence of "quiet" periods during a cycle is still not fully understood and would require meticulous modeling of heat and momentum transfers to the particle from the injection point to the detection volume. Time-resolved diagnostics in the "laser-illumination" mode also revealed periodic fluctuations in velocity and in the number of detected cold particles, but the latter with a modulation depth not as large as observed for the hot particles.

The fact that the two coatings, produced under similar net power in the plasma and in-flight average parameters, had different microstructures suggests that a control strategy of a plasma spray process, based only on maintaining the net power, temperature and velocity close to a predefined set-point, might, in some circumstances, be insufficient to guarantee coating reproducibility. One may argue that the conditions by which the coatings were produced were "extreme" and, moreover, atypical since the chosen conditions were outside the operating specifications of a F4-MB gun. Extreme spraying conditions were deliberately chosen in this study to determine whether the consistency of the coating microstructure is guaranteed when in-flight parameters and net plasma enthalpy are kept constant. It turns out that the impact of the plasma fluctuations can sometimes induce changes to the coating microstructure that are not accounted for in the in-flight characteristics. Note that significant changes in the amplitude of the fluctuations can also occur during the useful lifetime of electrodes due to electrode wear.[18] Hence, these results suggest that complementary indicators be added to in-flight particle temperature and velocity for guaranteeing consistent coating production. Future work will eventually tell which indicator, such as the voltage fluctuations, cold particle detection, particle jet orientation, and brightness monitoring, better assists in-flight temperature and velocity measurements for ensuring consistent coating production.

Acknowledgments

Special thanks to Gilles Mariaux (ENSIL, Limoges, France) for analyzing the alumina powder with the Microtrak technique. Technical support from Mario Lamontagne, Bruno Gauthier, and Sylvain Bélanger is truly acknowledged. The authors are also grateful to Basil Marple and Salim Bouaricha for proofreading the manuscript.

References

1. J.F. Bisson, B. Gauthier, and C. Moreau: "Effect of Plasma Fluctuations on In-Flight Particle Parameters," *J. Therm. Spray Technol.,* 2003, *12*(1), pp. 38-43.
2. G. Barbezat, F. Folio, C. Coddet and G. Montavon: "The Benefit of the PROTAL Process on the Adhesion of Thermal Sprayed Coatings" in *Thermal Spray: Surface Engineering via Applied Research*, C.C. Berndt, ed., ASM International, Materials Park, OH, 2000, pp. 57-62.
3. E.J. Kubel, Jr.: "Powders Dictate Thermal Spray Coating Properties," *Adv. Mater. Processes*, 1990, *12,* pp. 24-32.
4. J. Zierhut, P. Haslbeck, K.D. Landes, and G. Barbezat: "Triplex-An Innovative Three-Cathode Plasma Torch" in *Thermal Spray: Meeting the Challenges of the 21st Century*, C. Coddet, ed., ASM International, Materials Park, OH, 1998, pp. 1375-79.
5. G. Reiners, H. Kreye, and R. Scwetzke: "Properties and Characterization of Thermal Spray Coatings" in *Thermal Spray: Meeting the Challenges of the 21st Century*, C. Coddet, ed., ASM International, Materials Park, OH, 1998, pp. 629-34.
6. C. Moreau: "Towards a Better Control of Thermal Spray Processes" in *Thermal Spray: Meeting the Challenges of the 21st Century*, C. Coddet, ed., ASM International, Materials Park, OH, 1998, pp. 1681-93.

7. C. Moreau, P. Gougeon, M. Lamontagne, V. Lacasse, G. Vaudreuil, and P. Cielo: "On-Line Control of the Plasma Spraying Process by Monitoring the Temperature, Velocity, and Trajectory of the In-flight Particles" in *Thermal Spray Industrial Applications*, C.C. Berndt and S. Sampath, ed., ASM International, Materials Park, OH, 1994, pp. 431-36.
8. W.D. Swank, J.R. Fincke and D.C. Haggard: "A Particle Temperature Sensor for Monitoring and Control of the Thermal Spray Process" in *Thermal Spray: Science and Technology*, C.C. Berndt and S. Sampath, ed., ASM International, Materials Park, OH, 1995, pp. 111-16.
9. J. Vattulainen, J. Knuutila, T. Lehtinen, T. Mäntylä, and R. Hernberg: "In-Flight Particle Concentration and Velocity Measurements in Thermal Spraying Using Non-Intensified CCD Camera" in *Thermal Spray: Meeting the Challenge of the 21st Century,* C. Coddet, ed., ASM International, Materials Park, OH, 1998, pp. 767-72.
10. M. Vardelle, P. Fauchais, A. Vardelle, and A.C. Léger: "Thermal Spray, Influence of the Variation of Plasma Torch Parameters on Particle Melting and Solidification" in *A United Forum for Scientific and Technological Advances*, C.C. Berndt, ed., ASM International, Materials Park, OH, 1997, pp. 535-42.
11. M. Prystay, P. Gougeon, and C. Moreau: "Structure of Plasma-Sprayed Zirconia Coatings Tailored by Controlling the Temperature and Velocity of the Sprayed Particles," *J. of Thermal Spray Technol.*, 2001, *10*(1), pp. 67-75.
12. J. Madjeski: "Droplet Impact With a Cold Surface," *Int. J. Heat Mass Transfer,* 1983, *26,* pp. 1095-98.
13. J. Blain, F. Nadeau, L. Pouliot, C. Moreau, et al.: "Integrated Infrared Sensor System For On-Line Diagnostics of Particles Under Thermal Spraying Conditions," *Surf. Eng.*, 1997, *13,* pp. 420-24.
14. M. Pristay, P. Gougeon, and C. Moreau: "Structure of Plasma-Sprayed Zirconia Coatings Tailored by Controlling the Temperature and Velocity of the Sprayed Particles," *J. Thermal Spray Technol*., *10*(1), 2001, pp. 67-82.
15. Z. Duan and J. Heberlein: "Anode Boundary Layer Effects in Plasma Spray Torches" in *Thermal Spray: Surface Engineering via Applied Research*, C.C. Berndt, ed., ASM International, Materials Park, OH, 2000, pp. 1-7.
16. P. Gougeon, C. Moreau, V. Lacasse, M. Lamontagne, et al.: "A New Sensor for On-Line Diagnostics of Particles Under Thermal Spraying Conditions," *Adv. Process. Tech. Particulate Materials*, *6,* Metal Powder Industries Federation, Princeton, NJ, 1994, pp. 199-210.
17. L. Leblanc, C. Moreau, P. Gougeon, and J. Xi: "Long Term Stability of Plasma Spraying: Study on the Evolution of the In-Flight Particle State, Coating Microstructure, Voltage and Acoustic Signatures" in *Tagungsband Conference Proceedings,* E. Lugscheider and P.A. Kammer, ed., Pub. DVS Deutscher Verband für Schweissen, Germany, 1999, pp. 306-11.